

Dinosaur egg colour had a single evolutionary origin

Jasmina Wiemann^{1*}, Tzu-Ruei Yang² & Mark A. Norell³

Birds are the only living amniotes with coloured eggs^{1–4}, which have long been considered to be an avian innovation^{1,3}. A recent study has demonstrated the presence of both red-brown protoporphyrin IX and blue-green biliverdin⁵—the pigments responsible for all the variation in avian egg colour—in fossilized eggshell of a nonavian dinosaur⁶. This raises the fundamental question of whether modern birds inherited egg colour from their nonavian dinosaur ancestors, or whether egg colour evolved independently multiple times. Here we present a phylogenetic assessment of egg colour in nonavian dinosaurs. We applied high-resolution Raman microspectroscopy to eggshells that represent all of the major clades of dinosaurs, and found that egg colour pigments were preserved in all eumaniraptorans: egg colour had a single evolutionary origin in nonavian theropod dinosaurs. The absence of colour in ornithischian and sauropod eggs represents a true signal rather than a taphonomic artefact. Pigment surface maps revealed that nonavian eumaniraptoran eggs were spotted and speckled, and colour pattern diversity in these eggs approaches that in extant birds, which indicates that reproductive behaviours in nonavian dinosaurs were far more complex than previously known³. Depth profiles demonstrated identical mechanisms of pigment deposition in nonavian and avian dinosaur eggs. Birds were not the first amniotes to produce coloured eggs: as with many other characteristics^{7,8} this is an attribute that evolved deep within the dinosaur tree and long before the spectacular radiation of modern birds.

The huge diversity of avian egg colour⁹ has previously been attributed to the exploration of empty ecological niches after the extinction of nonavian dinosaurs at the terminal Cretaceous event¹. Different nesting environments, as well as nesting behaviours, are thought to influence egg colour^{10–12}. Egg colour may reflect selective pressure as a result of an ecological interaction between the egg producer and an egg predator (camouflage) or parasite (egg recognition). Avian egg colour has previously been shown to react in a plastic fashion to changes in the incubation strategy or climate, or even in mating behaviour^{1,10,12–18}. However, all previously proposed selective factors rely on the fact that the eggs are exposed to the environment^{10,11} and, with scant exception, not buried or covered. More-recent research suggests that egg colour may have co-evolved with (partially) open nesting habits in nonavian dinosaurs⁶ but offers only a single data point of egg colour outside crown birds, in open-nesting oviraptorid dinosaurs. Information on eggshell pigments in a larger sample of nonavian dinosaurs is required to understand the evolution of egg colour.

Both eggshell pigments—biliverdin and protoporphyrin IX—are tetrapyrroles with minor structural differences that affect their chemical properties and their distribution across the eggshell^{19–22}. In contrast to the more hydrophilic biliverdin, which extends deep into the prismatic zone of the eggshell, the more hydrophobic protoporphyrin—which causes spots and speckles—is restricted to the waxy cuticle^{21,23}. The different solubility properties of biliverdin and protoporphyrin appear to be key to their preservation potential^{6,21,22,24}. Protoporphyrin is more resilient to elution than biliverdin but both pigments are preserved in detectable trace amounts^{6,24}. Eggshell pigments appear to be restricted, if not bound, to the proteinaceous scaffold of the eggshell matrix²⁵.

Proteins transform during diagenesis into pyrrole-, pyridine- and imidazole-rich polymers through oxidative crosslinking²⁶; the resulting protein fossilization products (PFPs) appear similar to biliverdin and protoporphyrin IX in their chemical composition. Raman spectroscopy distinguishes between true egg-colour pigments and pigment-like PFPs²⁶ (Extended Data Fig. 1), and identifies and maps out pigments over eggshell surfaces and across vertical egg sections to characterize colour patterns and pigment deposition in fossil eggs. Placing this information in a phylogenetic context offers insights into whether egg colour evolved once within nonavian dinosaurs or multiple times independently, and might help to identify selective factors.

In our sample of nineteen archosaur eggshells, egg colour pigments are absent in eggshells of *Alligator mississippiensis*, the North American hadrosaurid *Maiaasaura peeblesorum*, the South American saltasaurid, the French titanosaurid and the North American troodontid (Fig. 1, Extended Data Figs. 2, 3). Egg colour pigments are preserved in eggshells from the oviraptorid *Heyuannia huangi*, Mongolian microtroodontids, the Chinese and Mongolian troodontids, the dromaeosaurid *Deinonychus antirrhopus*, the Mongolian enantiornithine, *Psammornis rothschildi*, *Rhea americana*, the North American ratite, *Dromaius novaehollandiae* and *Gallus domesticus* (Fig. 1, Extended Data Figs. 2, 3).

Only biliverdin was detected in *D. novaehollandiae*, whereas only protoporphyrin IX was present in the eggshells of the Mongolian microtroodontid (MAE 14-40 (specimen codes in parentheses)), the Chinese and Mongolian troodontids, the Mongolian enantiornithine, *P. rothschildi* and *G. domesticus*. Both egg colour pigments were detected in eggshells from *H. huangi*, the Mongolian microtroodontid (IGM 100/1323) and macrotroodontid (AMNH FARB 6631), *D. antirrhopus*, *R. americana* and the North American ratite. The presence of eggshell pigments corresponds to (partially) open nesting habits (Fig. 1).

All eggshell and associated sediment samples were plotted on a whole spectra-based principal component analysis (PCA) (Extended Data Fig. 4 and its Source Data). Principal component 1 (PC1, 57.118%) represents variability in pigment type, concentration and mode of eggshell alteration, whereas principal component 2 (PC2, 23.841%) separates samples into unpigmented and pigmented eggshells (Extended Data Fig. 5). The PCA (Extended Data Fig. 4a) revealed that eggshell biomolecules are distinct from organic material in the sediment, with both clusters separating across PC1 (73.116%). Within the eggshell cluster, extant and fossil materials are separated across PC2 (10.977%) (Extended Data Fig. 4a). A separate PCA (Extended Data Fig. 4b) based on the spectral fingerprint region of biliverdin and protoporphyrin IX (1,500 cm⁻¹–1,650 cm⁻¹ ± 2 cm⁻¹) included all fossil eggshell samples: the resulting chemo-space identified a characteristic cluster of pigmented eggshells, distinct from a separate cluster of unpigmented eggshells. Mapping protoporphyrin IX on the eggshell surface (Fig. 2a) demonstrated that the eggs of *H. huangi* were spotted, as were those of the Mongolian microtroodontids and troodontids, *D. antirrhopus*, and the Mongolian enantiornithine. Reconstructions of the egg colours are shown in Fig. 2a.

Depth profiles (Fig. 2b) across vertical eggshell sections show that pigments are absent in all layers of the *A. mississippiensis* eggshell as

¹Department of Geology & Geophysics, Yale University, New Haven, CT, USA. ²Steinmann Institute for Geology, Mineralogy, and Paleontology, University of Bonn, Bonn, Germany. ³Division of Vertebrate Paleontology, American Museum of Natural History, New York, NY, USA. *e-mail: jasmina.wiemann@yale.edu

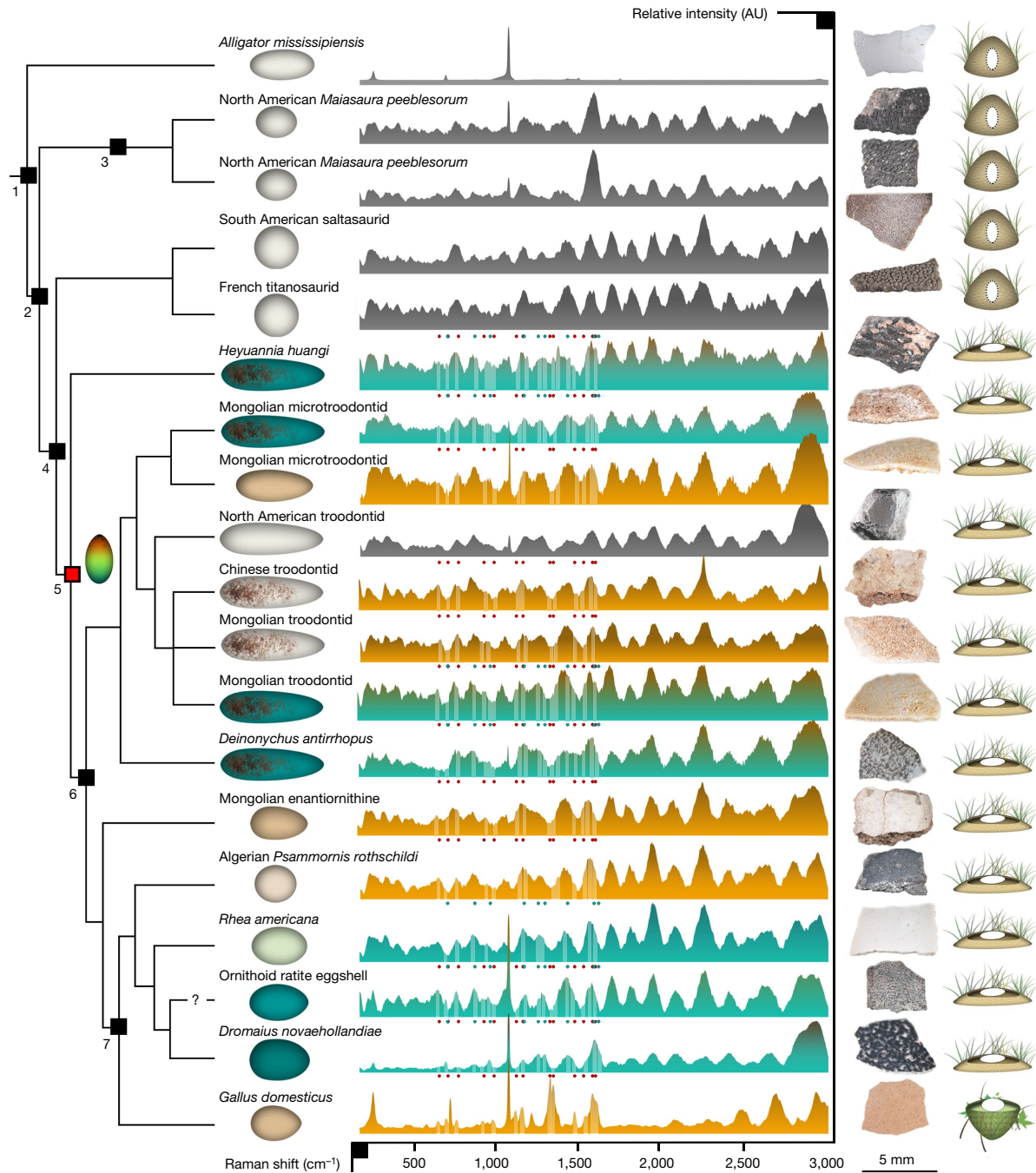


Fig. 1 | Stacked Raman spectra and ancestral state reconstruction on a pruned supertree. The Raman spectra represent bands at $200\text{--}3,000\text{ cm}^{-1} \pm 2\text{ cm}^{-1}$, from 6 accumulations and 20 s of exposure; spectra are baselined and normalized. Ancestral state reconstruction is based on published phylogenies^{8,28,29} ($n = 19$ sampled taxa), and maximum parsimony. The internal nodes are (1) Archosauria, (2) Dinosauria, (3) Ornithischia, (4) Saurischia, (5) Eumaniraptora, (6) Paraves and (7) Aves. The egg icon in the phylogeny labels Eumaniraptora. All terminal

taxa are represented by an icon indicating egg shape, and an example of reconstructed colour. If pigments are present, the area below the spectral function is coloured in blue (biliverdin) or orange (protoporphyrin IX), and all pigment bands are labelled with either blue (biliverdin) or red (protoporphyrin IX) dots. Relative Raman band intensities may vary owing to differential preservation. Photographs show the samples and nest icons encode three nesting strategies: buried, (partially) open ground and open tree nesting. AU, arbitrary units.

well as on the surface. The pigment stratification in *D. novaehollandiae*, *D. antirrhopus*, the Mongolian troodontid (AMNH FARB 6631) and *H. huangi* appears almost identical: in these samples, both pigments show a peak in concentration in the eggshell cuticle and increased concentration values through the entire prismatic zone. In the eggshells of *G. domesticus* and the Mongolian enantiornithine, the protoporphyrin IX signal reaches a peak in the organic and mineralized cuticle and extends into the uppermost prismatic zone. This is consistent with the absence of biliverdin in

the high-resolution point measurements of these samples. Only the Mongolian troodontid (AMNH FARB 6631) produced a different signal in the depth profiles to those obtained in the point measurements: in addition to very weak bands assigned to protoporphyrin IX in the point measurements for this eggshell, the depth profile revealed a weak biliverdin signal that is apparently restricted to the deeper eggshell layers. In contrast to the depth profiles in fresh *D. novaehollandiae* and *G. domesticus* eggshells, all fossil samples showed minor evidence of pigment elution (Fig. 2b). Only the Mongolian

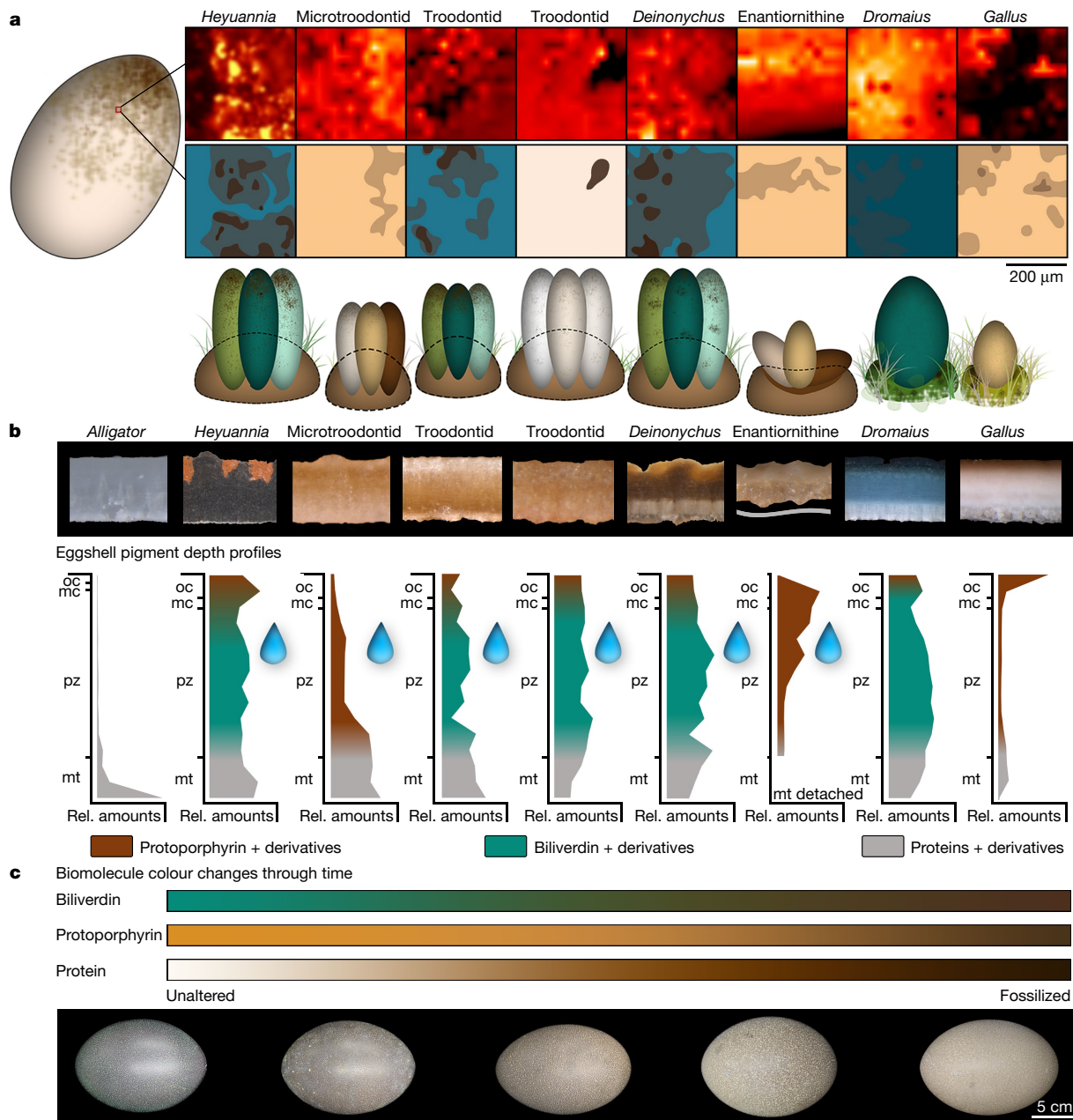


Fig. 2 | Egg colour reconstruction. **a**, Top, eggshell-pigment surface maps. $n = 8$; selection criteria were pigment presence (Fig. 1) and sufficient surface exposure. Protoporphyrin was mapped ($1,350 \text{ cm}^{-1} \pm 2 \text{ cm}^{-1}$, 2 accumulations, 5 s of exposure) with three independent repetitions, which yielded similar results. Increased signal intensity (yellow) is relative to the lowest signal intensity (black, which equals background noise in the absence of protoporphyrin IX). Bottom, egg reconstructions that combine information from panels above, **b** and Fig. 1 into a range of potential colours for the fossil eggshells. From left to right: *H. huangi*, Mongolian microtroodontid (MAE 14-40), Mongolian troodontid (AMNH FARB 6631), Mongolian troodontid (IGM 100/1003), *D. antirrhopus*, Mongolian enantiornithine, *D. novaehollandiae* and *G. domesticus*. **b**, Pigment depth

microtroodontid appeared to have experienced very intense pigment elution, as can be seen by comparing its depth profile to that of *G. domesticus* (protoporphyrin IX only, Fig. 2b). No trace of eggshell pigments was found in any of the sediment samples that surrounded the eggshells (Extended Data Fig. 6).

We infer endogeneity of the eggshell pigments detected on the basis of a number of criteria: the required 22 Raman band matches for biliverdin and protoporphyrin IX (Extended Data Fig. 1), the statistically supported separation of unpigmented and pigmented fossil eggshells

profiles across vertical sections of eggs from *A. mississippiensis*, plus the taxa shown in **a** ($n = 9$ specimens). Depth profiles were repeated three times independently, which yielded similar results. Photographs and depth profiles are not at the same scale. The distribution of protoporphyrin IX (red), biliverdin (blue) and proteinaceous matter (grey) is based on Raman point measurements and line maps ($1,166 \text{ cm}^{-1} \pm 2 \text{ cm}^{-1}$). Droplet icons indicate pigment elution. oc, organic cuticle; mc, mineralized cuticle; pz, prismatic zone; mt, membrana testacea. **c**, Visualization of gradual colour change of eggshell pigments and proteinaceous matter through time, based on observations of eggshells (*D. novaehollandiae* and *Casuaris casuaris*) and on a previous study²⁶.

(Extended Data Fig. 4b), the exclusion of pigment-like PFPs in the Raman-band identification (Extended Data Fig. 1), the similarity between pigment depth profiles in fresh and fossil eggshells (Fig. 2b) and the absence of pigments in the host sediments (Extended Data Figs. 4a, 6).

The phylogenetic distribution of egg colour within this archosaur sample supports a single evolutionary origin within nonavian theropod dinosaurs (Fig. 1). The homology between nonavian dinosaur and bird eggshell colour is further supported by an identical mode of eggshell

pigment deposition. This is based on a comparison of the depth profiles of eggshell pigments in nonavian eumaniraptorans with those of *D. novaehollandiae* and *G. domesticus*, which reveals that the stratification of pigments appears almost identical (Fig. 2) both among taxa that incorporate biliverdin and protoporphyrin IX and among taxa that incorporate only protoporphyrin IX. Only a larger sample of eggshell from taxa deeper in the tree will answer the question of whether egg colour is a true eumaniraptoran synapomorphy, or whether it evolved in more-basal theropods.

The North American troodontid is the only sample within eumaniraptorans⁸ that did not yield any colour signal. Although ornithischian *M. peeblesorum* eggshells from the same locality in the Two Medicine Formation also lacked colour, ornithoid ratite eggshells from comparable beds preserve traces of both biliverdin and protoporphyrin. We therefore interpret the absence of egg colour pigments in these troodontid eggshells (YPM VP PU 023259) as real, rather than taphonomic. Secondary reduction of egg colour is well-documented in modern birds and appears to be associated with increased sunlight exposure—an adaptation against overheating as seen, for example, in ostriches—nocturnality or cave breeding¹².

Our reconstructed egg colours (Fig. 2a) reflect the different preservation potential of biliverdin and protoporphyrin IX. We combined data from the high-resolution Raman point measurements, pigment surface maps and depth profiles of eggshell pigments (Fig. 2b). Because biliverdin is more likely to be washed out than the less-hydrophilic protoporphyrin IX, preserved traces of biliverdin indicate higher original concentrations⁶. Signs of elution are evident in all of our fossil eggshell samples, even though associated sediments lack detectable amounts of washed-out pigments (Extended Data Figs. 4a, 6). PFPs of the organic scaffold inside the eggshell produce a brownish-black colour²⁶ and original, unaltered eggshell pigments survive as traces through deep time⁶. It appears that part of the pigment fraction undergoes chemical alteration that contributes to a brownish discolouration (Fig. 2c).

The oviraptorid *H. huangi* belongs to the basalmost clade with coloured eggs (Fig. 1) in this study, and incorporates both biliverdin and protoporphyrin IX. It also represents the basalmost nonavian theropod group that built open nests—a transition that occurred at the base of Eumaniraptora and is found in nearly all its descendants^{6,27}. Absence of egg colour pigments in all taxa burying their eggs corroborates the hypothesis⁶ that egg colour co-evolved with open nesting habits (Fig. 1).

Egg colour is homologous in nonavian and avian dinosaur, and can be traced back to a single evolutionary origin in eumaniraptorans. The reconstructed diversity in egg colour and pattern (Fig. 2a) among nonavian dinosaurs (Fig. 1) mirrors that in extant birds^{1,3,5,18}. The evolution of spots and speckles in the eggshells of modern birds is often associated with individual recognition strategies in communally nesting groups, and intensively nest-parasitized host species¹⁸. Individual patterning of nonavian theropod eggs suggests the presence of much more complex nesting niches than previously recognized. Birds inherited a powerful molecular toolkit that enables them to colour their eggs; this discovery demands re-evaluation of evolutionary trends in egg colour at the base of modern birds.

Online content

Any methods, additional references, Nature Research reporting summaries, source data, statements of data availability and associated accession codes are available at <https://doi.org/10.1038/s41586-018-0646-5>.

Received: 6 March 2018; Accepted: 24 August 2018;

Published online 31 October 2018.

1. Kilner, R. M. The evolution of egg colour and patterning in birds. *Biol. Rev. Camb. Philos. Soc.* **81**, 383–406 (2006).
2. Cherry, M. I. & Gosler, A. G. Avian eggshell coloration: new perspectives on adaptive explanations. *Biol. J. Linn. Soc.* **100**, 753–762 (2010).
3. Cassey, P. et al. Why are birds' eggs colourful? Eggshell pigments co-vary with life-history and nesting ecology among British breeding non-passerine birds. *Biol. J. Linn. Soc.* **106**, 657–672 (2012).

4. Packard, M. J. & Seymour, R. S. in *Amniote Origins: Completing the Transition to Land* (eds Sumida, S. S. & Martin, K. L. M.) Ch. 8, 265–290 (Academic, San Diego, 1997).
5. Kennedy, G. Y. & Vevers, H. G. A survey of avian eggshell pigments. *Comp. Biochem. Physiol. B* **55**, 117–123 (1976).
6. Wiemann, J. et al. Dinosaur origin of egg color: oviraptors laid blue-green eggs. *PeerJ* **5**, e3706 (2017).
7. Norell, M. A., Clark, J. M., Chiappe, L. M. & Dashzeveg, D. A nesting dinosaur. *Nature* **378**, 774–776 (1995).
8. Turner, A. H., Makovicky, P. J., & Norell, M. A. A Review of dromaeosaurid systematics and paravian phylogeny. *Bull. Am. Mus. Nat. Hist.* **371**, 1–206 (2012).
9. Stoddard, M. C. & Prum, R. O. How colorful are birds? Evolution of the avian plumage color gamut. *Behav. Ecol.* **22**, 1042–1052 (2011).
10. Komdeur, J. & Kats, R. K. Predation risk affects trade-off between nest guarding and foraging in Seychelles warblers. *Behav. Ecol.* **10**, 648–658 (1999).
11. Gillis, H., Gauffre, B., Huot, R. & Bretagnolle, V. Vegetation height and egg coloration differentially affect predation rate and overheating risk: an experimental test mimicking a ground-nesting bird. *Can. J. Zool.* **90**, 694–703 (2012).
12. Hewitson, W. C. *Eggs of British Birds* (John Van Voorst, London, 1846).
13. Wallace, A. R. *Darwinism: An Exposition of the Theory of Natural Selection with Some of its Applications* (Macmillan, London, 1890).
14. Stoddard, M. C. et al. Camouflage and clutch survival in plovers and terns. *Sci. Rep.* **6**, 32059 (2016).
15. Newton, A. V. *A Dictionary of Birds* (A&C Black, London, 1896).
16. Ishikawa, S. et al. Photodynamic antimicrobial activity of avian eggshell pigments. *FEBS Lett.* **584**, 770–774 (2010).
17. Lahti, D. Population differentiation and rapid evolution of egg colour in accordance with solar radiation. *Auk* **125**, 796–802 (2008).
18. Gosler, A. G., Higham, J. P. & Reynolds, S. J. Why are birds' eggs speckled? *Ecol. Lett.* **8**, 1105–1113 (2005).
19. Ryter, S. W. & Tyrrell, R. M. The heme synthesis and degradation pathways: role in oxidant sensitivity. Heme oxygenase has both pro- and antioxidant properties. *Free Radic. Biol. Med.* **28**, 289–309 (2000).
20. Falk, J. E. *Porphyrins and Metalloporphyrins* (Elsevier, Amsterdam, 1964).
21. Gorchein, A., Lim, C. K. & Cassey, P. Extraction and analysis of colourful eggshell pigments using HPLC and HPLC/electrospray ionization tandem mass spectrometry. *Biomed. Chromatogr.* **23**, 602–606 (2009).
22. Milgrom, L. R. & Warren, M. J. in *The Colours of Life: An Introduction to the Chemistry of Porphyrins and Related Compounds* (ed. Milgrom, L. R.) Ch. 1–5, 1–175 (Oxford Univ. Press, Oxford, 1997).
23. Wang, X. T. et al. Comparison of the total amount of eggshell pigments in Dongxiang brown-shelled eggs and Dongxiang blue-shelled eggs. *Poult. Sci.* **88**, 1735–1739 (2009).
24. Igic, B. et al. Detecting pigments from colourful eggshells of extinct birds. *Chemoecology* **20**, 43–48 (2010).
25. Nys, Y., Gautron, J., Garcia-Ruiz, J. M. & Hincke, M. T. Avian eggshell mineralization: biochemical and functional characterization of matrix proteins. *C. R. Palevol* **3**, 549–562 (2004).
26. Wiemann, J. et al. Fossilization transforms proteins into N-heterocyclic polymers. *Nat. Commun.* <https://doi.org/10.1038/s41467-018-07013-3> (2018).
27. Varricchio, D. J. & Jackson, F. D. Reproduction in Mesozoic birds and evolution of the modern avian reproductive mode. *Auk* **133**, 654–684 (2016).
28. Sereno, P. C. The evolution of dinosaurs. *Science* **284**, 2137–2147 (1999).
29. Pisani, D., Yates, A. M., Langer, M. C. & Benton, M. J. A genus-level supertree of the Dinosauria. *Proc. R. Soc. Lond. B* **269**, 915–921 (2002).

Acknowledgements We thank D. E. G. Briggs for advice and assistance with the manuscript. M. Fabbri, N. Mongiardino Koch, J. Gauthier, K. Zykowski and R. Prum made helpful suggestions. Y.-N. Cheng, Y.-F. Shiao, X. Wu, T. Töpfer, P. M. Sander and K. Zykowski provided eggshell specimens. This research was supported by the Steven Cohen Award of the Society of Vertebrate Paleontology (J.W.), the Macaulay Family Endowment (M.A.N.) and the Division of Paleontology, American Museum of Natural History.

Reviewer information Nature thanks D. Zelenitsky and the other anonymous reviewer(s) for their contribution to the peer review of this work.

Author contributions J.W., T.-R.Y. and M.A.N. designed the research. J.W. designed and performed the experiments. M.A.N. and T.-R.Y. contributed materials. J.W. created the figures. J.W. and M.A.N. wrote the manuscript, which was reviewed by all authors.

Competing interests The authors declare no competing interests.

Additional information

Extended data is available for this paper at <https://doi.org/10.1038/s41586-018-0646-5>.

Supplementary information is available for this paper at <https://doi.org/10.1038/s41586-018-0646-5>.

Reprints and permissions information is available at <http://www.nature.com/reprints>.

Correspondence and requests for materials should be addressed to J.W. **Publisher's note:** Springer Nature remains neutral with regard to jurisdictional claims in published maps and institutional affiliations.

METHODS

No statistical methods were used to predetermine sample size. The experiments were not randomized and investigators were not blinded to allocation during experiments and outcome assessment.

We were able to rule out false-negative eggshell pigment assignments owing to taphonomic loss by including different available eggshell ($n = 19$) and sediment ($n = 12$) specimens from similar or identical host rocks. Every eggshell sample was blanked against its host-rock sediment to exclude false-positive results due to potential contamination (see Supplementary Information, chapters 1b–d, 3). The eggshell specimens cover extant *A. mississippiensis*, all major clades of extinct nonavian dinosaurs with multiple representatives, as well as extinct and extant palaeognath and neognath birds (Supplementary Table 2), and were taxonomically identified on the basis of their association with diagnostic adult, juvenile or embryonic skeletal remains or based on a combination of locality, diagnostic eggshell surface ornamentation and microstructure^{30,31} (Supplementary Information, chapter 2).

Eggshell and sediment samples (Supplementary Information, chapter 3) were imaged with a Leica MZ16 dissecting microscope (Optronics camera, LAS Core Software), surface-cleaned with ethanol and subjected to in situ Raman microspectroscopy. Raman spectroscopy was performed using a Horiba800 LabRam with 532-nm excitation (20 mW at the sample surface). The scattered Raman light was detected by an electron multiplier charged-coupled device after being dispersed with an 1,800-grooves-per-mm grating, and passed through a 100- μm entrance slit (hole size, 300 μm). The spectrometer was calibrated using the first-order Si band at 520.7 cm^{-1} . For point measurements (Fig. 1, Extended Data Fig. 1), 6 spectra were accumulated in the 300–2,000 cm^{-1} region for 20-s exposure time each. Fossil soft tissues containing PFPs were obtained from *Allosaurus fragilis* bone (YPM 48) and subjected to the same Raman point-measurement routine, to distinguish tetrapyrrole pigments from similar pigment-free PFPs (Extended Data Fig. 1). This process yielded 22 Raman bands (13 for protoporphyrin IX and 9 for biliverdin) that are diagnostic for egg colour pigments—including previously described pigment bands³²—in a potential PFP environment (Extended Data Fig. 1, Supplementary Information, chapter 1c, d). Further distinction of pigments from PFPs was aided by eggshell net enrichment plots (Extended Data Fig. 3). The eggshell pigments were mapped across eggshell surfaces and through vertical eggshell sections to image potential colour patterns, and to compare modes

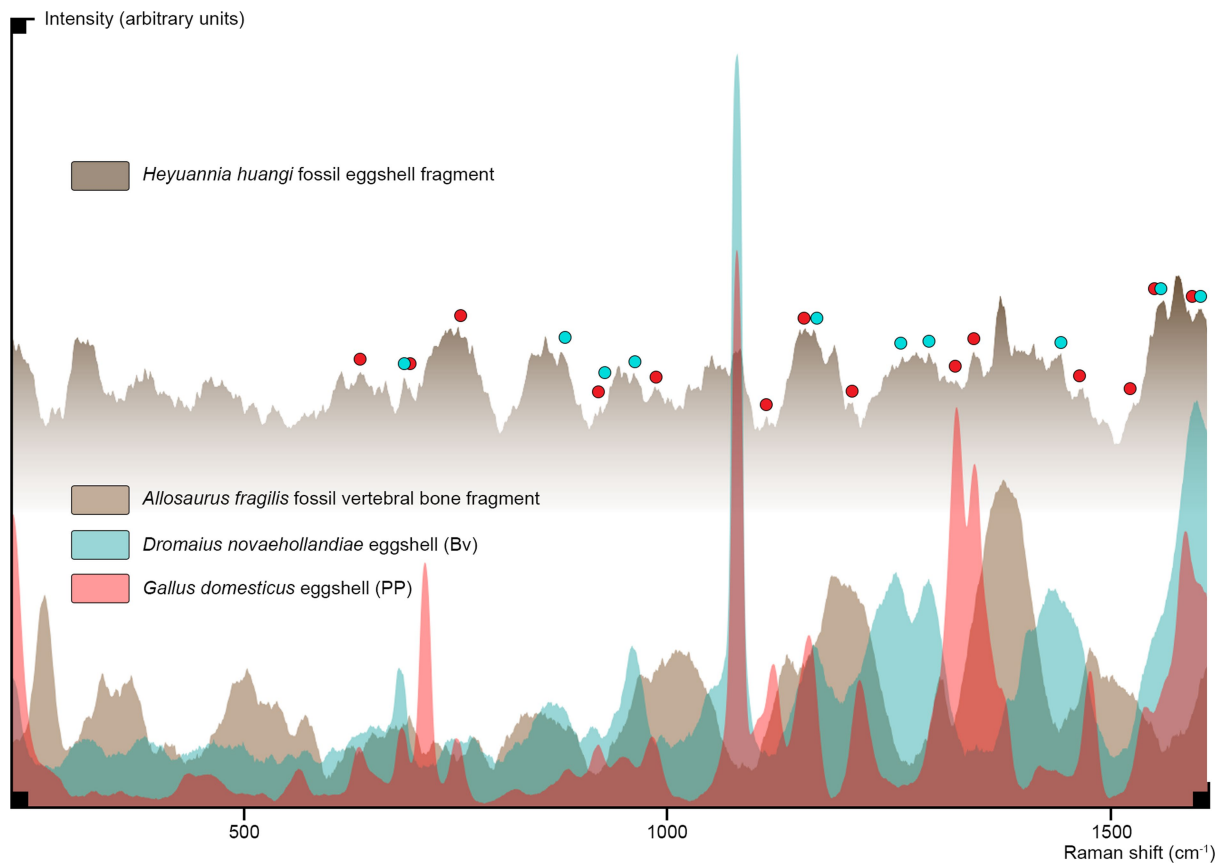
of pigment deposition among nonavian and avian dinosaurs. For pigment surface maps (Fig. 2) (protoporphyrin IX only, 1,350 cm^{-1}) and eggshell-pigment depth profiles (1,166 cm^{-1}), 2 spectra were accumulated over 5-s exposure time. Bands that represent protoporphyrin IX (at 1,350 cm^{-1} ; for surface mapping) and both pigments (at 1,166 cm^{-1} ; for depth profiling) were selected for their diagnostic molecular contents and signal intensity under the selected Raman parameters. The spectra were processed in Labspec 5 (spectral acquisition, mapping acquisition and standard spike removal) and subjected to a standard base-line correction (adaptive baseline, 50%, no offset and no smoothing) and standard normalization (based on the highest band in each spectrum) in SpectraGryph 1.2 spectroscopic software. Reconstructions of egg colours and patterns (Fig. 2a) represent combined data from point measurements, maps and depth profiles.

On the basis of the pigment data obtained for nonavian and avian dinosaurs, we performed a parsimony-based character tracing across our manually re-drawn composite phylogeny^{8,28,29} (pruned tree) in Mesquite 3.40 (coding: pigments absent = 0, pigment present = 1) (Extended Data Figs. 4, 6, Supplementary Information, chapter 4). Whole-spectra data of all eggshell and sediment samples (Extended Data Fig. 1), as well as extracted spectral data covering the pigment fingerprint region for fossil eggshells (Extended Data Fig. 1), were transformed into variance-covariance matrices (Extended Data Fig. 4 and its Source Data) and subjected to a PCA, which was performed in Past 3. Our study did not involve experiments that would require sample randomization or blinding of the investigators. **Reporting summary.** Further information on research design is available in the Nature Research Reporting Summary linked to this paper.

Data availability

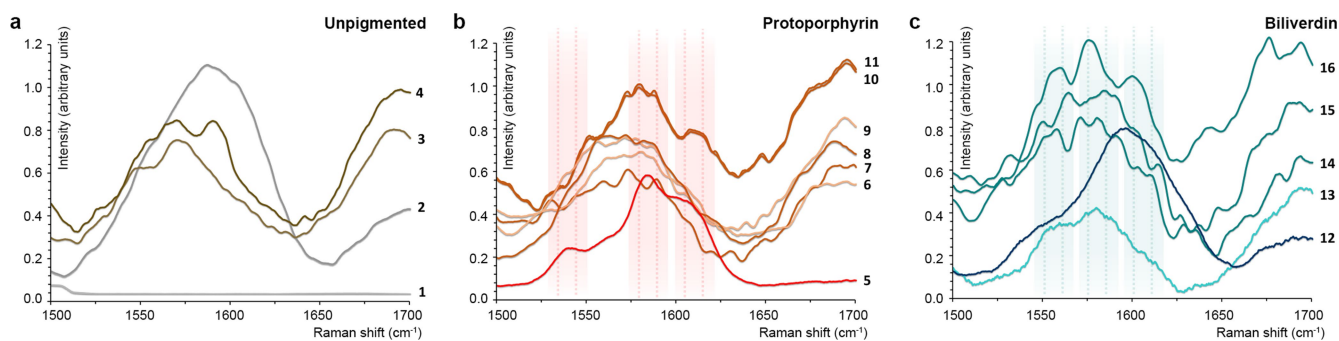
The authors declare that all Raman data supporting the findings of this study are available within the paper (pigment maps and depth profiles), and its Supplementary Information and Source Data.

- Carpenter, K. et al. (eds) *Dinosaur Eggs and Babies* (Cambridge Univ. Press, Cambridge, 1996).
- Mikhailov, K. E., Bray, E. S. & Hirsch, K. F. Parataxonomy of fossil egg remains (Veterovata): principles and applications. *J. Vertebr. Paleontol.* **16**, 763–769 (1996).
- Thomas, D. B. et al. Analysing avian eggshell pigments with Raman spectroscopy. *J. Exp. Biol.* **218**, 2670–2674 (2015).



Extended Data Fig. 1 | Spectral plots that validate the Raman bands indicative of biliverdin and protoporphyrin IX relative to PFPs, based on three representative samples. Spectral plots are $200\text{--}1,600\text{ cm}^{-1} \pm 2\text{ cm}^{-1}$, from 6 accumulations; spectra are baselined and normalized. Each spectrum was repeated three times independently, and yielded similar results. The lowermost spectral plot depicts blue spectra for biliverdin (from *D. novaehollandiae* eggshell), red spectra for protoporphyrin IX (from *G. domesticus*) and brown spectra for fossil

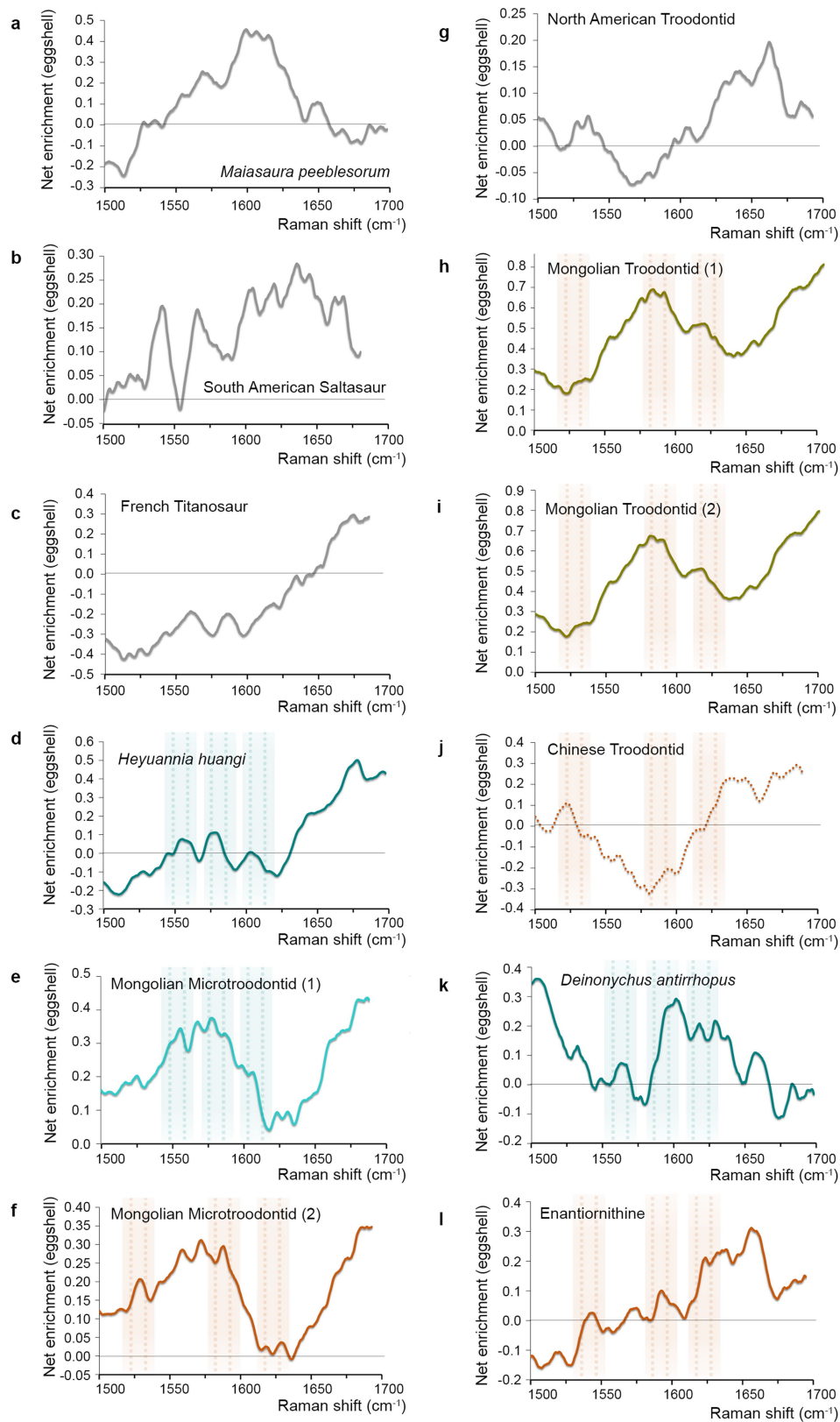
proteinaceous soft tissue (from *A. fragilis* bone; see previous study²⁶). The uppermost dark-brown spectra represent an in situ measurement for the *H. huangi* (NMNS CYN-2004-DINO-05) eggshell that is known to preserve both pigments (biliverdin and protoporphyrin IX). Blue asterisks label bands of biliverdin that differ from PFP; red asterisks label bands of protoporphyrin IX that are absent in fossil soft-tissue remains. Overall, 22 Raman bands are identified that can be generated only by original unaltered pigments, and not by PFPs that are simultaneously present.



Extended Data Fig. 2 | Spectral close-ups of the pigment fingerprint region for nineteen archosaur eggshells. Spectra are at $1,500\text{--}1,700\text{ cm}^{-1} \pm 2\text{ cm}^{-1}$ from 6 accumulations, and are baselined and normalized. **a**, Unpigmented eggshell samples (Fig. 1). **b**, Eggshell samples containing only protoporphyrin IX. Red bands label the set of bands that is diagnostic for protoporphyrin IX eggshell pigment. **c**, Biliverdin-rich eggshell samples. Blue bands label the set of bands that is diagnostic for biliverdin eggshell pigment. Note the characteristic spectral

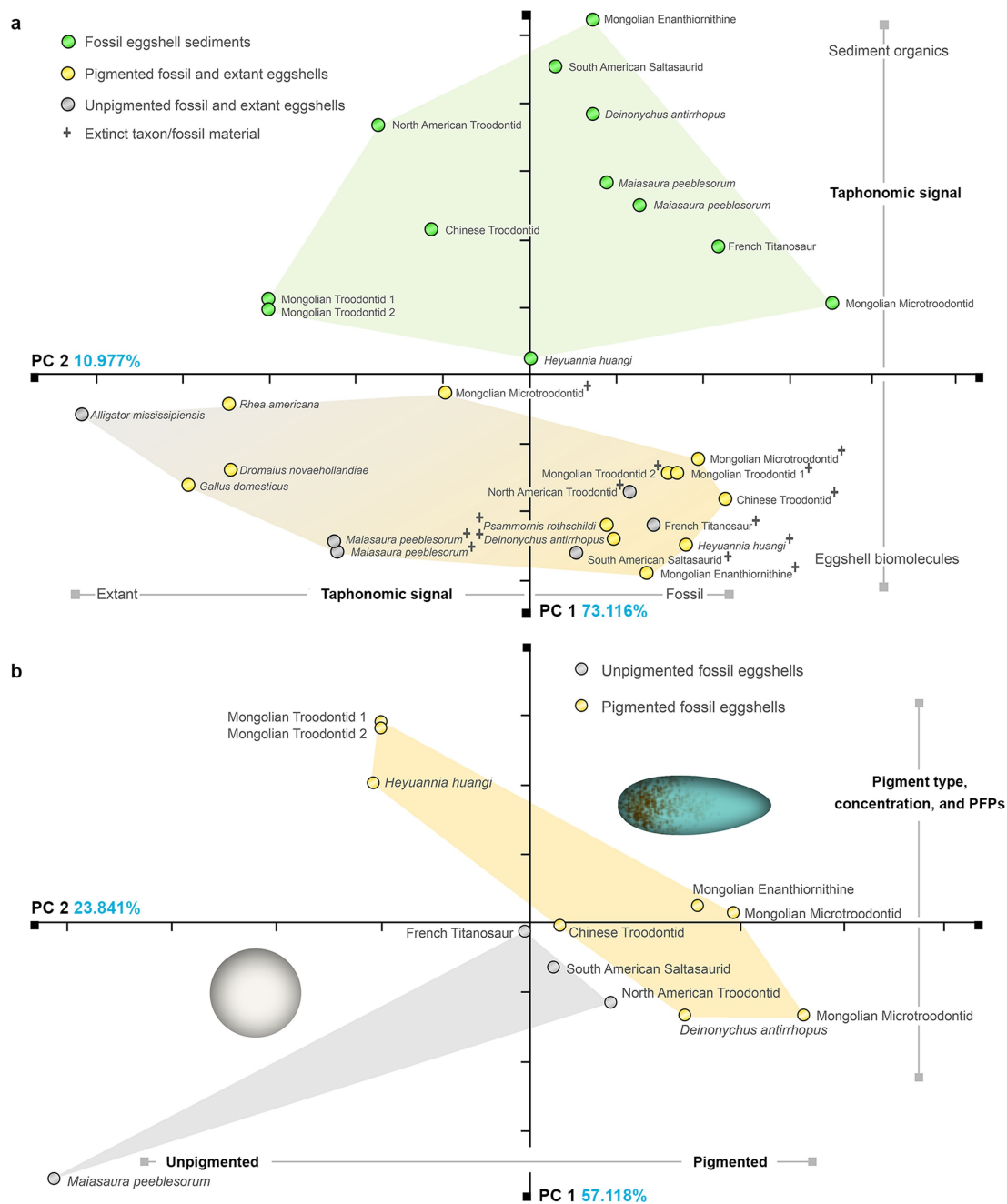
differences between unpigmented and pigmented eggshell samples.

1, *A. mississippiensis*; 2, *M. peeblesorum* (YPM VP PU 023464); 3, South American saltasaurid; 4, French titanosaurid; 5, *G. domesticus*; 6, Chinese troodontid; 7, Mongolian microtroodontid (MAE 14-40); 8, *P. rothschildi*; 9, Mongolian enantiornithine; 10, Mongolian troodontid (AMNH FARB 6631); 11, Mongolian troodontid (IGM 100/1003); 12, *D. noveahollandiae*; 13, *R. americana*; 14, *D. antirrhopus*; 15, Mongolian microtroodontid (IGM 100/1323); 16, *H. huangi*.



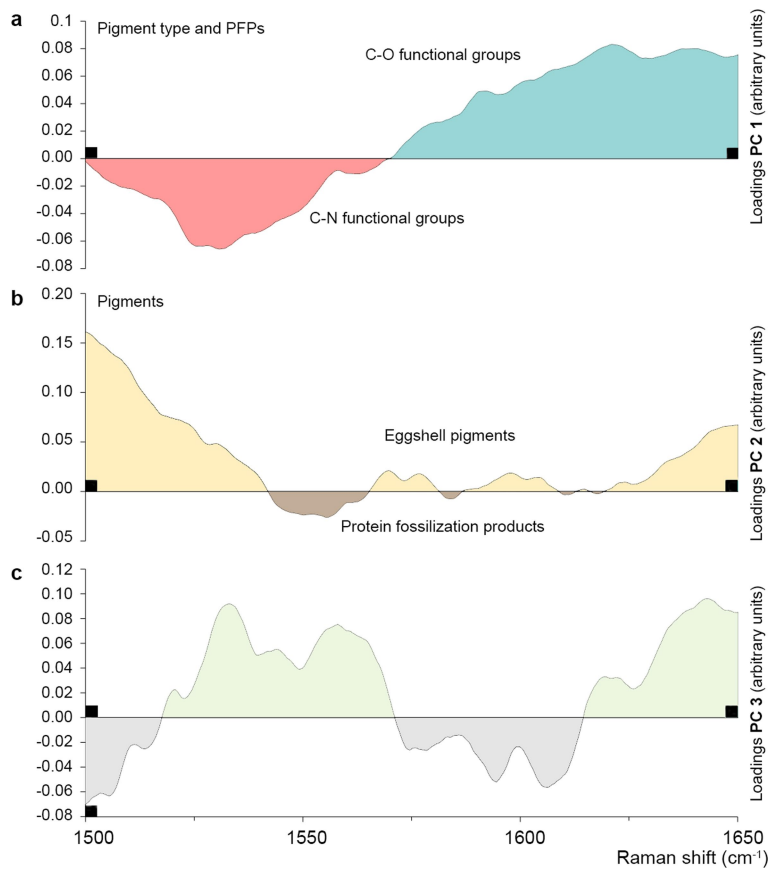
Extended Data Fig. 3 | Eggshell net enrichment plots resulting from subtraction of the sediment spectral functions from their corresponding eggshell spectral functions. Spectra are at $1,500\text{--}1,700\text{ cm}^{-1} \pm 2\text{ cm}^{-1}$ from 6 accumulations, and are base-lined and normalized. Positive values indicate a net enrichment of fossil eggshells in organic compounds relative to their sediment surroundings, whereas negative values indicate a net depletion. Red bands are diagnostic for

protoporphyrin IX, and blue bands are diagnostic for biliverdin. **a**, *M. peeblesorum* (YPM VP PU 023464). **b**, South American saltasaurid. **c**, French titanosaurid. **d**, *H. huangi*. **e**, Mongolian microtroodontid (IGM 100/1323). **f**, Mongolian microtroodontid (MAE 14-40). **g**, North American troodontid. **h**, Mongolian troodontid (AMNH FARB 6631). **i**, Mongolian troodontid (IGM 100/1003). **j**, Chinese troodontid. **k**, *D. antirrhopus*. **l**, Mongolian enantiornithine.



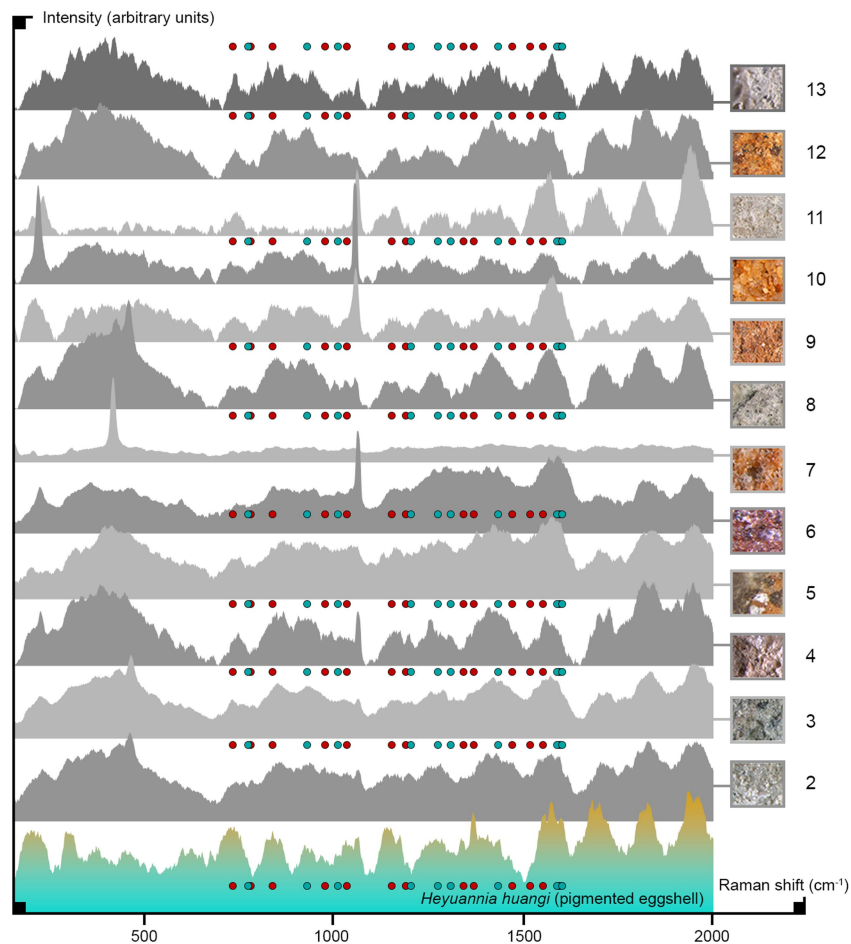
Extended Data Fig. 4 | PCA of spectral data. a, Whole spectra-based PCA of all modern ($n = 4$ biologically independent samples) and fossil ($n = 14$ biologically independent samples) eggshell and sediment samples ($n = 12$ independent samples). Sediment samples cluster together (green), and do not overlap the cluster of eggshell samples (grey-to-yellow). Eggshell biomolecules and sediment organics are distinct. Within the eggshell cluster, extant material is separated from fossil material. The proximity of unpigmented, protoporphyrin IX-bearing and biliverdin-rich extant eggshell material emphasizes that the taphonomic signal overprints the pigment signal at the level of a whole spectrum-based PCA. PC1 (73.116%) and PC2 (10.977%) are characterized by high support values and explain most of the variation in the eggshell and sediment sample set. **b**, PCA based on the pigment fingerprint region ($1,500\text{--}1,650\text{ cm}^{-1} \pm 2\text{ cm}^{-1}$) of protoporphyrin IX and biliverdin in

fossil eggshell material ($n = 12$ biologically independent samples). The exclusion of fresh and 'subfossil' (*P. rothschildi* and ornithoid ratite) eggshell material and the extraction of the pigment fingerprint region enable a chemo-space separation based on the eggshell pigment signal. Pigmented fossil eggshells form a cluster (yellow) that is separated from the cluster (grey) of unpigmented fossil eggshells (Extended Data Fig. 5). The pigment fingerprint region includes—besides protoporphyrin IX and biliverdin—structurally similar PFPs as well as pigment fossilization products, which account for the distribution of samples within each cluster of fossil eggshells (pigmented and unpigmented). PC1 represents sample variation based on pigment type, concentration and PFP contents, and PC2 separates samples based on the presence or absence of eggshell pigments (Extended Data Fig. 5).



Extended Data Fig. 5 | Loadings plots for principal component axes 1–3. These loading plots are for the PCA shown in Extended Data Fig. 4. **a**, Loadings per wavelength and functional group for PC1 (57.118%). Negative loadings are associated with C–N functions, while positive loadings are associated with C–O functions. PC1 separates samples in the chemospace based on pigment type (protoporphyrin IX ratio of C–N to C=O) > biliverdin (ratio of C–N to C=O)), concentration, and

PFP contents. **b**, Loadings per wavelength and functional group for PC2 (23.841%). Negative loadings are associated with prominent PFP bands, whereas positive loadings are associated with eggshell pigments. Thus, PC2 separates samples in the chemo-space on the basis of the presence or absence of eggshell pigments. **c**, Loadings per wavelength and functional group for PC3 (9.258%).



Extended Data Fig. 6 | High-resolution Raman point measurements of eggshell sediment samples. $n = 12$ independent samples. Measurement parameters are identical to those used to process eggshell samples, to guarantee comparability ($300\text{--}2,000\text{ cm}^{-1} \pm 2\text{ cm}^{-1}$, 6 accumulations, 20 s of exposure, base-lined and normalized). Each sediment measurement was repeated three times independently and yielded similar results. The coloured dots label potential pigment-band positions (biliverdin, blue; protoporphyrin IX red). For comparison, a pigment-positive spectrum of

H. huangi eggshell (1) is provided at the bottom, followed by sediments associated with *M. peeblesorum* (YPM VP PU 023464) (2); *M. peeblesorum* (YPM PU 22523) (3); South American saltasaurid (4); French titanosaurid (5); *H. huangi* (6); Mongolian microtroodontid (7); North American troodontid (8); Chinese troodontid (9); Mongolian troodontid (10); *D. antirrhopus* (11); Mongolian enantiornithine (12); and North American ornithoid ratite (13) eggshells. None of the sediments contains substantial amounts of eggshell pigments.

Reporting Summary

Nature Research wishes to improve the reproducibility of the work that we publish. This form provides structure for consistency and transparency in reporting. For further information on Nature Research policies, see [Authors & Referees](#) and the [Editorial Policy Checklist](#).

Statistical parameters

When statistical analyses are reported, confirm that the following items are present in the relevant location (e.g. figure legend, table legend, main text, or Methods section).

n/a Confirmed

- The exact sample size (n) for each experimental group/condition, given as a discrete number and unit of measurement
- An indication of whether measurements were taken from distinct samples or whether the same sample was measured repeatedly
- The statistical test(s) used AND whether they are one- or two-sided
Only common tests should be described solely by name; describe more complex techniques in the Methods section.
- A description of all covariates tested
- A description of any assumptions or corrections, such as tests of normality and adjustment for multiple comparisons
- A full description of the statistics including central tendency (e.g. means) or other basic estimates (e.g. regression coefficient) AND variation (e.g. standard deviation) or associated estimates of uncertainty (e.g. confidence intervals)
- For null hypothesis testing, the test statistic (e.g. F , t , r) with confidence intervals, effect sizes, degrees of freedom and P value noted
Give P values as exact values whenever suitable.
- For Bayesian analysis, information on the choice of priors and Markov chain Monte Carlo settings
- For hierarchical and complex designs, identification of the appropriate level for tests and full reporting of outcomes
- Estimates of effect sizes (e.g. Cohen's d , Pearson's r), indicating how they were calculated
- Clearly defined error bars
State explicitly what error bars represent (e.g. SD, SE, CI)

Our web collection on [statistics for biologists](#) may be useful.

Software and code

Policy information about [availability of computer code](#)

Data collection

Raman spectroscopic data were collected using LabSpec 5 software. Sample photographs were obtained using Leica LAS Core microscopic software.

Data analysis

Raman spectra were baselined and normalized in SpectraGryph 1.2, exported into Microsoft Excel and replotted. A Principal Component Analysis based on Raman data was performed in PAST 3. An ancestral state reconstruction based on a manually re-drawn composite phylogeny (pruned tree) including the $n=19$ biologically independent eggshell samples was performed in Mesquite 3.40. Compound figures were created in Photoshop CS5.

For manuscripts utilizing custom algorithms or software that are central to the research but not yet described in published literature, software must be made available to editors/reviewers upon request. We strongly encourage code deposition in a community repository (e.g. GitHub). See the Nature Research [guidelines for submitting code & software](#) for further information.

Data

Policy information about [availability of data](#)

All manuscripts must include a [data availability statement](#). This statement should provide the following information, where applicable:

- Accession codes, unique identifiers, or web links for publicly available datasets
- A list of figures that have associated raw data
- A description of any restrictions on data availability

The authors declare that all Raman data supporting the findings of this study are available within the paper (Fig. 2: pigment maps and depth profiles) and its supplementary information files (Source data for Fig. 1, Extended data Figs. 1, 2, 3, 6: Raman raw data). Additional PAST 3 files represent the raw data for the Extended data Figs. 4, and 5.

Field-specific reporting

Please select the best fit for your research. If you are not sure, read the appropriate sections before making your selection.

Life sciences Behavioural & social sciences Ecological, evolutionary & environmental sciences

For a reference copy of the document with all sections, see nature.com/authors/policies/ReportingSummary-flat.pdf

Ecological, evolutionary & environmental sciences study design

All studies must disclose on these points even when the disclosure is negative.

Study description

Our study investigates the evolution of egg colours in non-avian dinosaurs: Using overall 19 eggshell samples (including Alligator, non-avian dinosaur eggshell specimens, extinct and modern birds), we present the first phylogenetic assessment of non-avian dinosaur egg colour. Applying high-resolution Raman microspectroscopy point measurements to eggshells that represent all the major clades of dinosaurs, and the sediment control samples, we tested for preservation and endogeneity of the eggshell pigments biliverdin and protoporphyrin. Every sample was surface cleaned, and run at 6 accumulations over 20 s exposure time. Pigment samples were blanked against other organic compounds that commonly preserve in fossil eggshells. We found egg colour pigments preserved in all eumaniraptoran eggshells (except from a North American Troodontid), but none in the sediment control samples. Raman pigment surface maps (2 accumulations, 5 s exposure) revealed that the coloured eggs were spotted and speckled. Raman pigment depth profiles demonstrated an identical mechanism of pigment deposition in pigmented nonavian and avian dinosaur eggs. Absence of colour in ornithischian and sauropod eggs represents a true signal rather than a taphonomic artefact. An ancestral state reconstruction using the obtained pigment data on a pruned tree that includes all sampled taxa shows that egg colour had a single evolutionary origin in non-avian theropod dinosaurs. The diversity in colour and pattern of non-avian eumaniraptoran eggshells challenges that known from modern birds, indicating far more complex reproductive behaviours in non-avian dinosaurs than previously known. Even though long thought, crown birds did not evolve egg colours, but inherited them from their nonavian dinosaur ancestors.

Research sample

A total of nineteen eggshell specimens and twelve adhering sediment samples were included in the eggshell pigment Raman point measurements. All samples represent museum specimens: Alligator mississippiensis eggshell (YPM uncat), Maiasaura peeblesorum eggshell (YPM VP PU 023464) and (YPM PU 22523), Saltasaurid eggshell (STIPB E360), Hypselosaurus priscus eggshell (YPM PU 21158), Heyuannia huangi eggshell (NMNS CYN-2004-DINO-05), Microtroodontid eggshell (IGM 11/1323) and (MAE 14-40), Troodontid eggshell (YPM VP PU 023259), and (PFMM-0014003517), and (FARB 6631), and (IGM 100/1003), Deinonychus antirrhopus eggshell (AMNH 3015), Enantiornithine eggshell (IGM 100/1339), Psammornis rothschildi eggshell (ZFMK 23a:III/c/23), Rhea americana eggshell (YPM ORN 24444), Ornithoid ratite eggshells (YPM PU 22594), Dromaius novaehollandiae eggshells (YPM ORN 24447), and Gallus domesticus eggshells (YPM ORN 23146). All of these specimens are housed either at the Yale Peabody Museum, at the American Museum of Natural History, at the Steinmann Institute Bonn, or the Zoological Research Museum Koenig Bonn. One additional tern eggshell was used to calibrate the Raman mapping routine (YPM uncat), shown in Fig. S2. Further five egg specimens from the YPM ornithological collection were photographed to illustrate pigment color changes through time. These eggs represent the taxa Dromaius novaehollandiae and Casuarius casuarius (YPM 1994, YPM 133667, YPM 141992, YPM 141998, YPM 142001, YPM 142002) and are shown in Fig. 2c.

Sampling strategy

No sample size calculation was performed. The nineteen eggshell samples, and the twelve sediment samples were chosen based on available coverage of the cladogram. We generally sampled one specimen per genus, except from Maiasaura which is covered by two biologically independent eggshell samples per genus. The sampled genera offer multiple representatives for every major branch of nonavian dinosaurs and allow to draw reliable conclusions about general evolutionary trends in nonavian dinosaur egg color evolution: Two samples cover ornithischian dinosaurs, two additional samples cover sauropod dinosaurs, nine samples cover nonavian eumaniraptoran dinosaurs, and five samples cover modern birds. Eggshells of Maiasaura represent the only ornithischian eggshells which are taxonomically assigned based on embryonic remains in their eggs. Within sauropods we sampled based on specimen availability. Since previous research suggests egg color in oviraptorids, we compiled a comprehensive theropod eggshell sample. We cover one oviraptorid, two microtroodontids, four troodontids, the only discovered deinonychosaurian eggshell, and one enantiornithine eggshell, as well as two extinct ratites, and two modern birds. Our samples offer also multiple representatives per "taphonomic environment", to rule out false negative, taphonomy-based pigment assignments. Six samples cover limestone host rocks (Maiasaura (n=2), South American Saltasaur, North American Troodontid, Deinonychus, ornithoid ratite eggshell), while other nine samples cover sand/siltstones (French Titanosaur, Heyuannia, Microtroodontids (n=2), Troodontids (n=3), Enantiornithine, Psammornis). Based on the sampling of comparable taphonomic environments, qualitative conclusions of pigmentation are backed up against potential taphonomic biases: Both host rock types cover eggshells with and without eggshell pigments, what suggests that

pigments can survive in both taphonomic environments, and corroborates that eggshells without evidence for pigmentation were originally unpigmented, and did not lose their pigments through taphonomic processes.

Data collection

Mark Norell and Tzu-Ruei Yang provided all eggshell and sediment specimens which are not part of the Yale Peabody collection (YPM). Jasmina Wiemann cleaned all eggshells with ethanol prior to any measurements. She also imaged all specimens and sediments (Leica MZ16 dissecting microscope with Optronics camera, LAS Core Software), and performed the Raman spectroscopy high-resolution point measurements, pigment surface maps, and depth profiles (recorded using LabSpec 5 and a Horiba LabRam 800) at Yale University. Jasmina Wiemann baselined and normalized all acquired spectra in SpectraGryph 1.2. Tzu-Ruei Yang corroborated Raman-based findings for some of the samples at the Steinmann Institute. Jasmina Wiemann, Tzu-Ruei Yang, and Mark Norell evaluated the data, and Jasmina Wiemann performed the statistical analyses in PAST 3, and the ancestral state reconstruction based on a manually re-drawn composite phylogeny including all nineteen sampled taxa in Mesquite 3.40. Jasmina Wiemann created the composite figures in Photoshop CS5. All authors interpreted the findings and wrote the manuscript.

Timing and spatial scale

Our eggshell and sediment museum specimens cover localities from all over the world (please see Supplementary Table 2 for details). The sample set was built from 2015 to 2017. All samples were imaged, and measured consecutively, from August 2017 to January 2018. Since all investigated specimens are accessioned in museums, not active sample collection was conducted in this study.

Data exclusions

All Raman point measurements for the total of 31 sample specimens are included in the manuscript and its Supplementary Information. Nineteen eggshell samples were included in the Raman point measurements. From this sample pool 8 samples fulfilled the criteria of an exposed, smooth surface area, and a substantial protoporphyrin pigment signal, necessary for eggshell pigment surface mapping (spots and speckles are based only on protoporphyrin). All of these samples were included into the eggshell pigment depth profiles, in addition to one unpigmented Alligator sample as control sample. All eggshell and sediment samples are included in the Principal Component Analysis shown in Extended data Fig. 4a, while only fossil eggshells are included in the second Principal Components Analysis shown in Extended data Fig. 4b. Reasoning for the exclusion of extant and "subfossil" eggshells here is the reduction of taphonomic noise in the chemospace to extract the pigment signal.

Reproducibility

Every Raman measurement presented in the main text Figs. and the Extended data Figs., point/map/depth profile, was repeated three times (technical replicates) independently and yielded similar, if not identical results. None of the sediment samples showed evidence for eggshell pigments, while all tested eumamiraptoran eggshells, except from the North American Troodontid, yielded evidence for pigmentation. All attempts at replication of these results were successful.

Randomization

Randomization cannot be applied to this study, because Raman spectra are characteristic for every sample, and can be taxonomically assigned at a glance based on their unique and distinctive taphonomic and compositional signatures. Also, we do not use any statistics that would require randomization. Samples were grouped together based on their identity (eggshell versus sediment), and their age (extant versus fossil). The Principal Component Analysis shown in the Extended data Fig. 4b suggests that fossil eggshells group as unpigmented eggshells, and pigmented eggshells.

Blinding

Blinding is not relevant to this study, because Raman spectra are characteristic for every sample, and can be taxonomically assigned at a glance based on their unique and distinctive taphonomic and compositional signatures. However, all eggshell and sediment spectra were analysed "blind" without any preliminary expectation towards the analytical outcome of pigment detection.

Did the study involve field work? Yes No

Reporting for specific materials, systems and methods

Materials & experimental systems

- | | |
|-------------------------------------|--|
| n/a | Involved in the study |
| <input checked="" type="checkbox"/> | <input type="checkbox"/> Unique biological materials |
| <input checked="" type="checkbox"/> | <input type="checkbox"/> Antibodies |
| <input checked="" type="checkbox"/> | <input type="checkbox"/> Eukaryotic cell lines |
| <input type="checkbox"/> | <input checked="" type="checkbox"/> Palaeontology |
| <input checked="" type="checkbox"/> | <input type="checkbox"/> Animals and other organisms |
| <input checked="" type="checkbox"/> | <input type="checkbox"/> Human research participants |

Methods

- | | |
|-------------------------------------|---|
| n/a | Involved in the study |
| <input checked="" type="checkbox"/> | <input type="checkbox"/> ChIP-seq |
| <input checked="" type="checkbox"/> | <input type="checkbox"/> Flow cytometry |
| <input checked="" type="checkbox"/> | <input type="checkbox"/> MRI-based neuroimaging |

Palaeontology

Specimen provenance

Alligator (extant, FL, US), Maiasaura, North American Troodontid, ornithoid ratite egg (Cretaceous, MT, US), Saltasaurid (Cretaceous, Argentina), French titanosaur (Cretaceous, France), Heyuannia and Chinese Troodontid (Cretaceous, China), Microtroodontids, Mongolian Troodontids, Enantiornithine (Cretaceous, Mongolia), Deinonychus (Cretaceous, MT, US), Psammornis (Quaternary, Algeria), Rhea and Dromaius (extant, MT, US), Gallus (extant, CT, US).

Specimen deposition

All unique fossil materials presented in our study are stored in the collections of the Yale Peabody Museum, the American Museum of Natural History, the Steinmann Institute for Paleontology, and the Zoological Research Museum Koenig, and are readily available for examination. Please see "Research sample" in this Reporting Summary for the catalogue numbers.

Dating methods

No new dates are provided.

Tick this box to confirm that the raw and calibrated dates are available in the paper or in Supplementary Information.